QUID 2017, pp. 888-896, Special Issue N°1- ISSN: 1692-343X, Medellín-Colombia

NUMERICAL STUDY OF PARAFFIN HEAT TRANSFER IN MELTING PROCESS IN SOLAR WATER HEATER STORAGE TANK

(Recibido el 15-06-2017. Aprobado el 04-09-2017)

Pouya Pedram Azad
Islamic Azad University, *MA student of mechanical engineering, Nour Branch, Iran, pouyapedram1@gmail.com*

Hesamoddin Salarian
Islamic Azad University, *Assistant professor, mechanical engineering, Nour branch, Iran, H_salaryan@yahoo.com*

Abstract. In this paper, we have studied paraffin heat transfer in melting process in solar water heater storage tanks by numerical investigation. We have used Gambit software for geometrical production. The output of this software has been used as the input for ANSYS Fluent. We have also used SIMPLE algorithm for solving algebraic equations. As for momentum equations we have used second-order upstream discretion and for other alternatives including kinetic energy and turbulence loss and finite volume transfer equation we have used first-order upstream discretion. The results show that the average heat goes up by the increase in the number of fins and reduces the melting time of phase change material (PCM). Also with the increase in the length of the fins more quantity of the material changes phases and turns into liquid. With the increase in thickness of the fins, minimal increase is seen in phase change of the material and its liquidation.

Keywords: Heat transfer, melting process, solar water heater, storage tank, paraffin

Citar, estilo APA: Azad, P. & Salarian, H. (2017). Numerical study of paraffin heat transfer in melting process in solar water heater storage tank. *Revista QUID (Special Issue)*, 888-896.

1. INTRODUCTION

So far many research works have been conducted on investigating heat transfer in various systems for storage of energy.

Ravikumar et al. (2008) studies phase change material as thermal energy storage material for cooling system of buildings and presented three methods. They concluded that the stored heat and cold are only used when needed not automatically. Nashina and Takahira (2009) used $10H_{20}$ and Na_2SO_4 PCM for performance analysis of a latent heat storage system with phase change material for newly designed solar collectors in greenhouse heating. They found out that 40-60 percent of PCM latent heat potential can be freed. This is where almost almost half of the PCM is not used.

The latent thermal energy storage in PCM is a method that has gained momentum during the recent decades. These researches have been theoretically and in experimental level carried out on thermal energy storage in PCM in various geometries. Sayoto and Herwits (n. d) theoretically and experimentally studied PCM thermal storage latently in circular capsules. Biyezli and Ramanaroyan (2007) have studied a numerical model for investigating thermodynamic response of a PCM balls by using formulation of separate phases mono-dimensionally. Labat et al. (2008) designed a sample thermal transformer containing PCM experimentally for generating 1KW thermal power within two hours (i.e. storage of 2kWh energy). They tested the transformer in a closed circuit wind tunnel to get the fixed airflow movement rate under thermal changes, so that PCM was allowed to melt and then solidify. They measured temperature and speed for eight airflow rates and calculated the thermal power of the transformer. Mostafa et al. (2012) studied latent thermal storage of PCM in various applications including air conditioning systems. They studied modeling of PCM solidification in a shell and tube finned thermal storage. They conducted a comparative study of PCM solidification in the rectangular shell of the same volume and heat transfer, and found out that the PCM solidification rate in thermal storage in cylindrical shell is higher than the rectangular shell. Dolado et al. (2011). The simulated expanded models studied the thermal energy storage performance in a PCM-air thermal transformer in real scale both numerically and experimentally. They also evaluated the analysis of heat transfer between air and other phase change materials in commercial microcapsules. Wang and Yang (2011) studied the three-dimensional transient numerical simulation for cooling by using PCM in multi-fin heat sink. The results showed that the expanded theory model was well corresponding to between the numerical predictions and experimental data. They found out that the transient temperature with a deviation of 10.2 percent has been predicted. Shalaby et al. (2014). studied solar dryers with PCM as energy storage medium and found out that using solar dryers with PCM reduces thermal loss and improves productivity of the system. Guelpa et al. (2013) studied entropy generation analysis for the design improvement of a latent heat storage system. In their studies they used computational fluid dynamics (CFD) to study the phenomenon of phase change in PCM by entropy. Mehrali et al (2013) prepared a form-stable composite PCMs by vacuum impregnating paraffin into graphene oxide sheets and the composite PCMs contained 48.3 wt.% of paraffin without leakage of melted PCM. Gracia and Cabeza (2015) has shown that thermal energy storage (TES) is a way to do so, but also other purposes can be pursued when using TES in buildings, such as peak shaving or increase of energy efficiency in HVAC systems. Gracia and Cabeza (2015) reviews TES in buildings using sensible, latent heat and thermochemical energy storage. Sustainable heating and cooling with TES in buildings can be achieved through passive systems in building envelopes, Phase Change Materials (PCM) in active systems, sorption systems, and seasonal storage.

Gao, et. al (2017) reported the design and fabrication of bifunctional microcapsules for solar photocatalysis and solar thermal energy storage by using cuprous oxide (Cu2O) as an inorganic shell to encapsulate a paraffin-type phase change material (PCM), n-eicosane. Such a new type of microcapsules was synthesized successfully by using an emulsion templating self-assembly method along with in-situ precipitation. The chemical structures of the resultant microcapsules were determined by Fourier-transform infrared spectroscopy, and the elemental distributions of microcapsule shell were confirmed by X–ray photoelectron spectroscopy and energy-dispersive X–ray spectroscopy. The scanning and transmission electronic microscopic observations demonstrated that the microstructures and morphologies of microcapsules were influenced significantly by the surfactant and alkali concentrations as well as the portion of cupper source for the synthesis. After the synthetic condition was optimized, the obtained microcapsules exhibited an interesting octahedral morphology and a typical core-shell structure. The thermal analysis results suggested that the microcapsules synthesized at the optimum condition not only obtained high encapsulation and energy-storage efficiencies but also presented a high thermal stability and phase-change reliability. Most of all, the microcapsules obtained a solar thermal energy-storage capability through solar photo thermal conversion and also exhibited a high solar photo catalytic activity to organic dyes under the sunlight illumination. In addition, the microcapsules showed a gas-sensitive feature to some harmful organic gases in the presence of Cu_2O shell. The microcapsules developed by this work indeed reveal a bifunctional feature derived from both the core and the shell materials and thus show a great potential for industrial and domestic applications due to their extended functions.

Tang, et al. (2017) fabricated three types of polyethylene glycol (PEG) based shape-stabilized PCMs with various pore structures of EG, AC and ordered mesoporous carbon (CMK-5). The highest content of PEG without leakage was about 70 wt.% for AC, 90 wt.% for both EG and CMK-5, respectively.

Kahwaji, et. al (2017) present a comprehensive study of thermal and related properties (transition temperature, transition enthalpy change, heat capacity, thermal conductivity, thermal diffusivity, density), thermal stability (on cycling through the transition up to 3000 times) and chemical stability (when in contact with 16 common containment materials at 75 °C) for six organic phase change materials: decanoic acid (aka capric acid, [CH3(CH2)8COOH]), dodecanoic acid (aka lauric acid, [CH3(CH2)10COOH]), tetradecanoic acid (aka myristic acid, [CH3(CH2)12COOH]), hexadecanoic acid (aka palmitic acid, [CH3(CH2)14COOH]), octadecanoic acid (aka stearic acid, [CH3(CH2)16COOH]) and 1-octadecanol ([CH3(CH2)17OH]). All show melting transitions in the temperature range 30–70 °C which is suitable for solar thermal applications, with substantial enthalpy changes (> 145 J g-1), and all are thermally stable over 3000 cycles. These materials all have significant potential for solar thermal energy storage applications.

2. PROBLEM STATEMENT

The problem under investigation is two-dimensional, transient and with natural displacement. There is no input-output boundary in the problem. The left and right walls as well as the fins have fixed temperature. The upper and lower walls are both nonconductive. The zone holding paraffin change material acts as fluid zone and another zone as fin, defined as solid zone with copper solidification material in which heat transfer will take place. In Fig. 1, the three-dimensional geometry has been displayed.

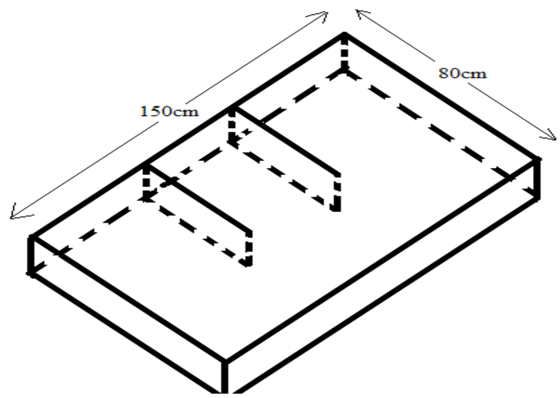

Figure 1. Three-dimensional geometry

3. BASIC GOVERNING EQUATIONS

The equations governing fluids indicate the physical laws for conservation in the form of mathematical phrases, some of which are the following:

1- Fluid mass always remains fixed.

2- The degree of changes in the motion is equal to the resultant forces on the fluid particles (Newton’s second law)

3- The change in the internal energy of a closed system is equal to the amount of heat supplied to the system, minus the amount of work done by the system on its surroundings (first law of thermodynamics).

3-1- Mass Conservation Equation

The first law governing fluid particle is the mass conservation law. Considering the equilibrium of the mass for a fluid element, this law can be expressed in this way that the net motion rate of input mass to the fluid element is equal to the mass increase rate in the fluid element, i.e. considering a fluid element we can write (Graciaa & Cabeza, 2015):

$$\frac{\partial \rho}{\partial t} + \frac{\partial(\rho u)}{\partial x} + \frac{\partial(\rho v)}{\partial y} + \frac{\partial(\rho w)}{\partial z} = 0 \qquad (1)$$

Where u, v and w are the elements of resultant speed and p is the density of the fluid.

3-2- Momentum Conservation Equations for Free Displacement Motion

These equations, called Navier-Stocks Equations can be written in the following way:

$$\frac{\partial(\rho u)}{\partial t} + div(\rho u U) = -\frac{\partial P}{\partial x} + div\big(\mu . grad(u)\big) + S_{Mx}$$

$$\frac{\partial(\rho v)}{\partial t} + div(\rho v U) = -\frac{\partial P}{\partial y} + div\big(\mu . grad(v)\big) + S_{My}$$

$$\frac{\partial(\rho w)}{\partial t} + div(\rho w U) = -\frac{\partial P}{\partial z} + div\big(\mu . grad(w)\big) + S_{Mz} \qquad (2)$$

P is the static pressure on the fluid. Without considering details of the forces imposed on the body, the general impact of these forces can be considered in the form of SMi for the size of motion along i in volume and time specified in which i includes directions x, y or z. The body force includes only the gravity force:

$$S_{Mx} = S_{My} = 0, S_{Mz} = -\rho g \qquad (3)$$

3-3- Energy Equation for Fluid Motion

With respect to the free displacement model the energy equation can be presented as the following:

$$\partial_t(ph) + \partial_t(p\Delta H) + \partial_i(pu_i h) = \partial_i(k \partial_i T) \qquad (4)$$

Where h is sensible enthalpy and ΔH is latent enthalpy.

3-4- numerical simulation

As for validation and verification, this study was compared with the experimental finding of Kamkari & Shokouhmand (2014) and as Figure 2 shows, there is a good correspondence. They made an experimental investigation of PCM melting in rectangular enclosures with and without fin.

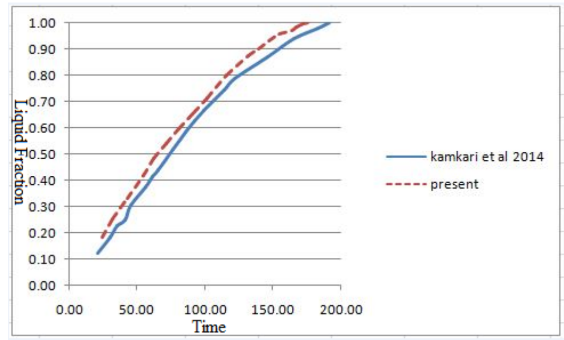

Figure 2. A comparison of the findings of this study with Kamkari & Shokouhmand experiment

The boundary conditions governing the two studies were almost the same so that upper and lower walls were nonconductive and the right and left walls had fixed temperature. The fins were placed on the left wall. The experiment in three temperatures of 55, 60 and 70 centigrade were carried out for with and without fin. In their work, the visual study of melting process along with qualitative and quantitative data on melting had been carried out by using digital photos and simultaneous investigation of completion of the melting process and recording temperature in the middle plate of water heater. They came to the conclusion that with the increase in the fins, unheated area (the area shown in blue in the following diagram) diminishes. In the end, they extracted the experimental relation of Nusselt number and liquid fraction based on dimensionless parameters. (Kamkari & Shokouhmand, 2014) In terms of parameters, we used numerical investigation method and in terms of results (due to presentation of a detailed report on the degree of reduction of the time of melting) and boundary conditions this work is distinctive from previous works.

First normal scaffolding was carried out on the body. With respect to the results (density, pressure and free surface modeling), meshes on the body were 0.1 mm in size and rectangular. (Figure 3) Due to geometry of the structure we used a square of scaffolding with submap elements.

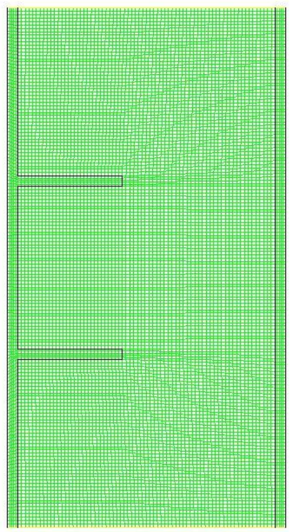

Figure 3. Productive scaffolds on the model

After controlling the performance of the program it is necessary to investigate independence of answers from the total number of points in the scaffolding in order to find an appropriate solution network. To study the process of independence from the network, the issue was studied in four scaffolding positions. With respect to Table 1, it is clear that almost for all smaller networks it is identical in 12843 answers. Therefore, the total number of elements used were 12843 for implementation of the project. A comparison of the time of melting it was observed that almost 3/06 percent of fault is seen in the answers in scaffolding.

Table 1: Studying independence of network

Grid point	8972	10345	12843	13400
Liquid Fraction = 1	3832	3844	3860	3869

4. RESULTS

4-1- Investigating the Impact of Fin Number

Fig. 4 depicts the impact of increasing the number of fins on the melting time. As it is shown, the melting time is reduced with the increase in the number of fins. It can be understood from this figure that melting time for Case A (finless) is around 3860 seconds. Considering this as the basis for melting time, the other cases can be also calculated. According to estimations the reduced melting time for Case B is equal to 71 percent. Also it is understood that the increase in the number of fins has considerable impact on the melting time of PCM, specifically in case of increased number of fins. Such an impact is due to the fact that an increase in the number of fins boosts the surface contact with heat transfer and more heat is transferred to the material.

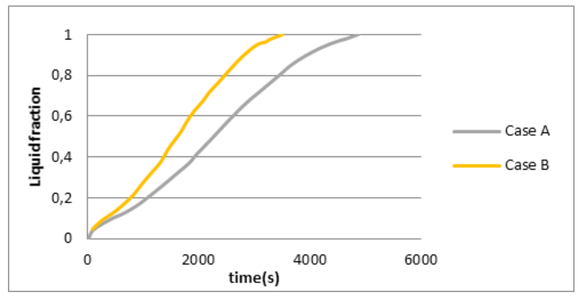

Figure 4. Impact of the number of fins on melting time

Fig. 5 displays distribution of temperature based on the number of fins for cases A and B after 1000 seconds. It is seen that the average temperature goes up by an increase in the number of fins and thus reduces the melting time for PCM. Heat transfer between hot surface of transformer and the PCM surface occurs through heat transfer displacement and in the upper section of the fins a thin layer is formed and with the passage of time this layer becomes thicker and causes liquid fraction. The heated liquid moves up as a result of the difference in density, therefore, it is a sign of natural heat transfer displacement.

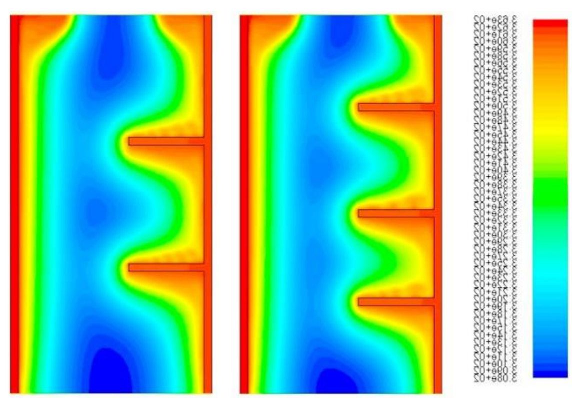

Case B Case A

Figure 5. Temperature contour after 1000 seconds based on the number of fins

Fig. 6 displays distribution of liquid fraction in the phase change process based on the changes in the number of fins for cases A and B. With the increase in the number of fins, a greater portion of PCM changes into liquid.

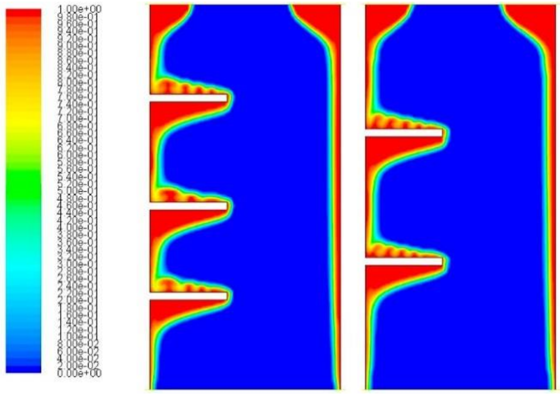

Figure 6. Liquid fraction contour after 1000 seconds based on the number of fins

In Fig. 7, as an instance, the results related to 1000, 2000 and 3000 seconds for liquid fraction have been shown. As shown, it is proceeding into the area.

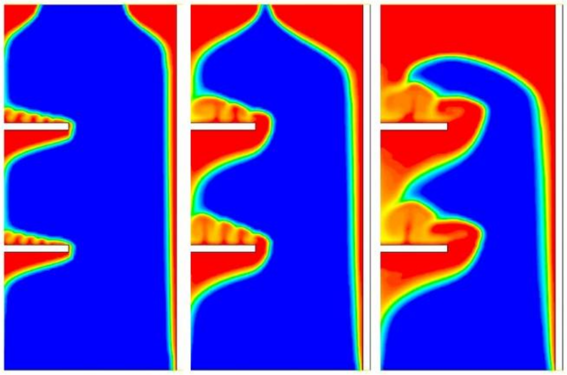

Figure 7. Liquid fraction contour for various time spans

4-2- Studying Impact of Fin Length

Fig. 8 shows the length of the fins. As it is seen, the increase in the length of the fins reduces the melting time. The full melting time for case A is 3860 seconds. For other cases in lengths of 3, 4 and 5 cm we can get 61%, 48% and 74% respectively. Also it can be understood that the length of fins has a considerable effect on the melting time of PCM. Such an impact is due to the fact that an increase in the number of fins boosts the surface contact with heat transfer and more heat is transferred to the material. Figure 9 shows temperature distribution based on the changes in fin length for Case B in lengths of 3, 4 and 5 cm for 1000 seconds.

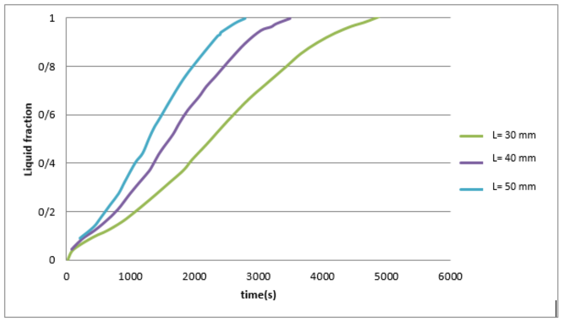

Figure 8. Impact of fin length on reducing of melting time

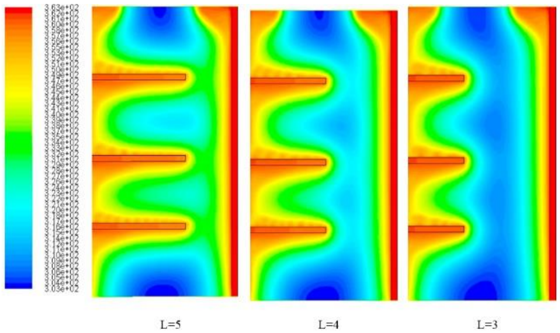

Figure 9. Temperature contour after 1000 seconds based on the increase in fin lengths

Fig. 10 shows liquid fraction distribution in phase change process based on the changes in fin length for Case B in lengths of 3 to 5 some 1000 seconds into the melting process. With the increase in the number of fins, greater portion of material changes phase and turns into liquid.

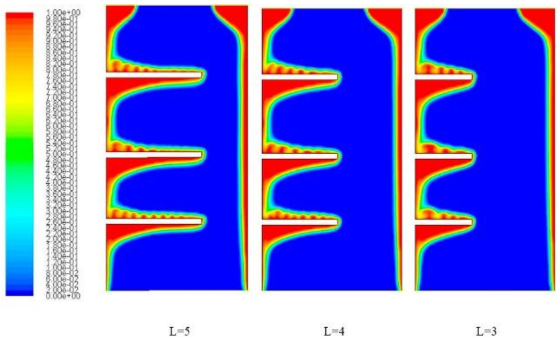

Figure 10. Liquid fraction after 1000 seconds based on increasing the length of fins

4-3- Studying Thickness of the Fins

Fig. 11 shows the impact of increase in the thickness of the fins on melting time in PCM. As it is shown, with the increase in thickness of fins, the melting time falls down. With respect to this figure it is understood that the total time needed for melting in Case A is 7060 seconds. For other cases in thicknesses of 3, 5 and 8 mm we can get 36%, 40% and 45% respectively. Also it can be understood that the thickness of fins has no considerable effect on the melting time of PCM. Therefore, using thicker fins increases heat transfer only.

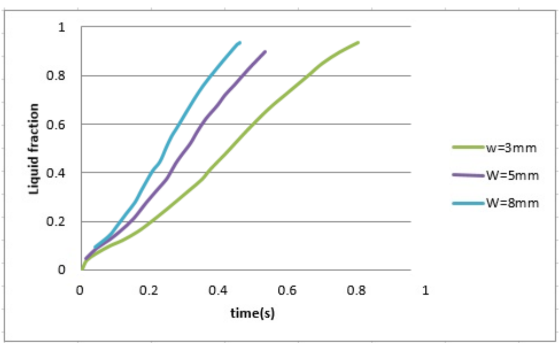

Figure 11. Impact of increase in thickness of the fins on reducing melting time

Fig. 12 shows temperature distribution based on the change in thickness of the fins in Case A in thicknesses of 3, 5 and 8 mm after 1000 seconds. As it is seen, the average temperature goes a little high with the increase in the thickness of the fins and the resulting reduction in melting time is trivial.

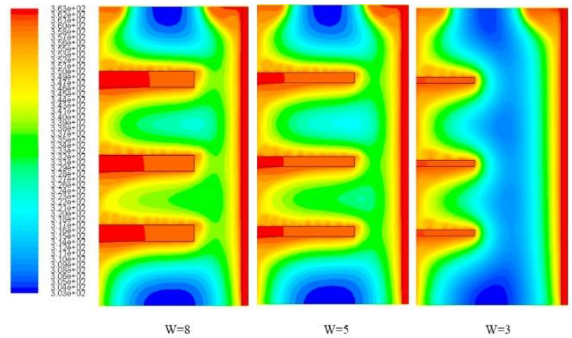

Figure 12. Temperature contour after 1000 seconds based on increase in thickness of the fins

Fig. 13 shows the distribution of liquid fraction taking place in phase change process based on changes in the thickness for Case B in thickness of 3, 5 and 8 mm 1000 seconds after the start of melting process. Upon the increase in thickness of the fins, a trivial boost in the PCM liquidation rate is observed.

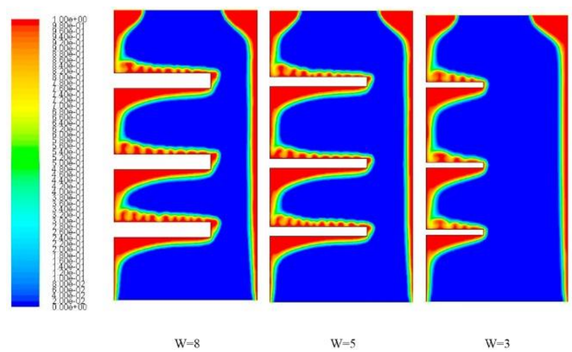

Figure 13. Liquid fraction contour after 1000 seconds based on an increase in the thickness of fins

5. CONCLUSION

In this paper, the numerical study of paraffin heat transfer in melting process of solar water heater storage tank was investigated. We used Gambit software for geometrical production. The output of this software has been used as the input for ANSYS Fluent. We also used SIMPLE algorithm for solving algebraic equations. As for momentum equations we used second-order upstream discretion and for other alternatives including kinetic energy and turbulence loss and finite volume transfer equation we have used first-order upstream discretion. The results were the following:

1- The increase in the number of fins has a considerable effect on melting time of the PCM.

2- The average temperature goes high with the increase in the number of fins, thus reduces the time needed for PCM melting.

3- The increase in the length of the fins has a considerable effect on PCM melting time.

4- The increase in the number of fins has brought about more liquidation of PCM.

5- The average temperature goes a little high with the increase in the thickness of fins, but reduces the time needed for PCM melting insignificantly.

6- With the increase in the thickness of the fins, a trivial increase in PCM liquidation is observed.

REFERENCES

Biyezli, Z, Ramanaroyan, F. (2007). Modeling of Phase change material Peak Load Shifting. Energy and building, 39(3), 289-305

Dolado, P., Lazaro, A. Marin, J. Zalba, B. (2011). Characterization of melting and solidification in a real scale PCM-air heat exchanger: Numerical model and experimental validation, Energy Conversion and Management 52, 1890–1907, 2011.

Gao, F., Wang, X. & Wu, D. (2017). Design and fabrication of bifunctional microcapsules for solar thermal energy storage and solar photocatalysis by encapsulating paraffin phase change material into cuprous oxide, Solar Energy Materials and Solar Cells, 168, 146–164.

Graciaa, A. & Cabeza, L. (2015). Phase change materials and thermal energy storage for buildings, Energy and Buildings (2015).

Guelpa, E., Sciacovelli, A. & Verda, V. (2013). Entropy generation analysis for the design improvement of a latent heat storage system, Energy, 53,128-138.

Kahwajia, S., Johnsonb, M., Kheirabadic, A., Groulxb, D. & White, M. (2017). Fatty acids and related phase change materials for reliable thermal energy storage at moderate temperatures, Solar Energy Materials and Solar Cells, 167,109–120.

Kamkari, B. & Shokouhmand, H. (2014). Experimental investigation of phase change material melting in rectangular enclosures with horizontal partial fins, International Journal of Heat and Mass Transfer, 78, 839-851.

Labat, M. Virgone, J. David, D. & Kuznik F, (2008). Experimental assessment of a PCM to air heat exchanger storage system for building ventilation application. DOI: 10.1016/j.applthermaleng.x.02.025

Mehrali, M., Latibari, S.T., Mehrali, M., Metselaar, H.S. & Silakhori, M. (2013). Shapestabilized phase change materials with high thermal conductivity based on paraffin/graphene oxide composite. Energy Convers Manage, 67, 275–82.

Mosaffa, A.H. Talati, F. Tabrizi, H. & Rosen, M.A. (2012). Analytical modeling of PCM solidification in a shell and tube finned thermal storage for air conditioning systems, Energy and Buildings, 49, 356–361.

Nashina, Y. & Takahira, R. K. (2009). Performance analysis of a latent heat storage system with phase change material for new designed solar collectors in greenhouse heating. Solar Energy, 83(12), 2109-2119,

Ravikumar, M. & Srinivasan, PSS. (2008) Phase Change Material as a Thermal Energy Storage Material for Cooling of Building. Journal of Theoretical and Applied Information Technology, 503-511.

Sayoto, D.F. & Herwits, R.J. (n. d). PCM thermal storage in buildings: A state of art, 13, 123-127

Shalaby, S.M., Bek, M.A. & El-Sebaii, A.A. (2014). Solar dryers with PCM as energy storage medium: A review, Renewable and Sustainable Energy Reviews, 33, 110–116.

Tang, L., Yang, J., Bao, R., Liu. Z., Xie, B. Yang, M., Yang, W. (2017). Polyethylene glycol/graphene oxide aerogel shape-stabilized phase change materials for photo-to-thermal energy conversion and storage via tuning the oxidation degree of graphene oxide, Energy Conversion and Management, 146, 253-264

Yi-Hsien Wang & Yue-Tzu Yang, (2011). Three-dimensional transient cooling simulations of a portable electronic device using PCM (phase

change materials) in multi-fin heat sink, Energy,
36, 5214-5224.